

1        **BCG overexpressing an endogenous STING agonist provides**  
2                    **enhanced protection against pulmonary tuberculosis**

3  
4        **Ruchi Jain Dey<sup>1,3#</sup>, Bappaditya Dey<sup>1,4#</sup>, Alok Kumar Singh<sup>1</sup>, Monali Praharaj<sup>1,2</sup> and**  
5        **William Bishai<sup>1\*</sup>**

6        <sup>1</sup>Center for Tuberculosis Research, Johns Hopkins University School of Medicine,  
7        Baltimore, Maryland, USA

8        <sup>2</sup> Department of Microbiology and Molecular Immunology, Johns Hopkins Bloomberg  
9        School of Public Health, Baltimore, Maryland, USA

10        # These authors have equally contributed to the work.

11

12

13        Current address:

14        <sup>3</sup>Department of Biological Sciences, BITS Pilani-Hyderabad, Hyderabad, Telangana,  
15        India

16        <sup>4</sup>National Institute of Animal Biotechnology, Hyderabad, Telangana, India

17

18

19        \*To whom correspondence should be addressed at Johns Hopkins School of Medicine,  
20        1550 Orleans Street, Baltimore, MD 21287. Phone: 410-955-3507; Email:

21        [wbishai@jhmi.edu](mailto:wbishai@jhmi.edu)

22

23 **ABSTRACT**

24  
25 Stimulator of interferon genes (STING) has emerged as a key signaling receptor that  
26 induces proinflammatory cytokines, and small molecule STING agonists are being  
27 developed as anticancer and antiviral agents. Here we report a strategy of delivering a  
28 STING agonist from within live BCG. We generated a recombinant BCG (BCG-*disA*-OE)  
29 that overexpresses the endogenous mycobacterial diadenylate cyclase gene and  
30 releases high levels of the STING agonist c-di-AMP. In macrophages BCG-*disA*-OE  
31 elicited statistically significantly stronger TNF- $\alpha$ , IL-6, IL-1 $\beta$ , IRF3, and IFN- $\beta$  levels than  
32 BCG-WT. In a 24-week guinea pig vaccination-*Mtb* challenge model, BCG-*disA*-OE  
33 reduced lung weights, pathology scores, and *Mtb* CFU counts in lungs by 28% ( $p < 0.05$ ),  
34 34%, and 2.0 log<sub>10</sub> CFU units ( $p < 0.5$ ) compared with BCG-WT, respectively.  
35 Overproduction of the STING agonist c-di-AMP significantly enhanced the protective  
36 efficacy of BCG against pulmonary and extrapulmonary tuberculosis. Our findings  
37 support the development of BCG-vectored STING agonists as a TB vaccine strategy.

## 38 INTRODUCTION

39           Recent studies have identified a key role for the stimulator of interferon genes  
40 (STING) intracellular sensor in mediating innate immune responses cellular stress or  
41 pathogen infection [1,2]. STING is a cytosolic receptor for both pathogen-associated  
42 molecular pattern (PAMP) molecules such as cyclic dinucleotides c-di-AMP or c-di-GMP  
43 produced by bacteria, and for mammalian endogenous danger signaling DAMP  
44 molecules such as 2',3' cyclic GMP-AMP (cGAMP) which is synthesized by cGAS (cyclic  
45 GMP-AMP synthase) in response to microbial or self-derived cytosolic double-stranded  
46 DNA [1-4]. Activation of STING induces numerous interferon-stimulated genes including  
47 type I interferons (IFN $\alpha/\beta$ ) and is associated with co-activation of NF- $\kappa$ B and STAT6  
48 transcription factors that follows or parallels the induction of interferon regulatory factors  
49 (IRF) transcription factors. Thus endogenous and exogenous cyclic dinucleotides (CDNs)  
50 are strong TLR-independent mediators of innate host defenses [5,6]. Based on the key  
51 role of STING signaling, pharmacological stimulation of the pathway using small molecule  
52 STING agonists is currently being tested for enhancement of antitumor immunity and as  
53 potential anti-viral therapy [5,7].

54           As they are capable of inducing potent cytokine and cellular immune responses  
55 against pathogens, CDN STING agonists also exhibit attractive vaccine adjuvant  
56 properties. They increase expression of MHC class II, co-stimulatory molecules  
57 (CD80/CD86) as well as activation (CD40) and adhesion (CD45) markers; in addition  
58 STING agonists have been shown to enhance antigen processing and presentation to T  
59 cells [8-10]. Among microbial-derived CDNs, c-di-AMP has emerged as an efficient  
60 activator of macrophages and leads to robust Th1, Th17 and CD8 T cell responses [11].

61 Efforts to harness small molecule CDNs themselves as vaccine adjuvants to  
62 enhance systemic immunity, however, may be limited by rapid systemic clearance and  
63 by the fact that as negatively charged molecules, CDNs do not effectively cross cell  
64 membranes of macrophages and professional antigen presenting cells [6]. Hence there  
65 is a need to develop a cost-effective formulations of CDNs and related STING agonists  
66 that allow for sustained release to the cytosolic compartment of antigen-presenting cells.

67 Our previous findings showed that *Mycobacterium tuberculosis* (*Mtb*), an  
68 intracellular pathogen, possesses di-adenylate cyclase enzyme, *disA* (MT3692), that  
69 synthesizes and secretes c-di-AMP into the host cell cytosol. We showed that an *Mtb*  
70 strain engineered to overexpress c-di-AMP (*Mtb-disA-OE*) was significantly attenuated in  
71 lethality, ability to proliferate, and cause disease pathology in a mouse model [12]. In a  
72 separate study, we showed that mutation of the *cdnP* gene encoding a cyclic dinucleotide  
73 phosphodiesterase (CdnP) that hydrolyzes c-di-AMP lead to a mutant *Mtb* strain that  
74 accumulates c-di-AMP and is similarly attenuated for virulence [13].

75 Based on these results we constructed a c-di-AMP–overexpressing bacillus  
76 Calmette–Guérin (BCG), an attenuated strain of *Mycobacterium bovis* widely used as a  
77 TB vaccine globally, and found that it induced a significantly higher IRF and IFN- $\beta$   
78 response than BCG itself, indicating that bacterial-derived c-di-AMP gains access to the  
79 host cell cytosol despite the fact that BCG lacks the ESX-1 protein secretion system found  
80 in *Mtb*. These findings strongly encouraged us to evaluate whether BCG-induced immune  
81 responses against TB are boosted by overexpression of the STING agonist c-di-AMP.

82 A number of candidate vaccines for TB are currently being evaluated in clinical  
83 trials, prime boost strategies that include BCG have failed to show improved protective

84 efficacy in humans over BCG alone [14]. In the paper we report the development of a  
85 recombinant BCG which is boosted by endogenous overexpression of a STING agonist.  
86 This c-di-AMP–overexpressing recombinant BCG strain (BCG-*disA*-OE) exhibited  
87 increased IRF induction, IFN- $\beta$  synthesis, and release of the pro-inflammatory cytokines  
88 IL-6, TNF $\alpha$  and IL1 $\beta$  in vitro than were observed with BCG-WT. Importantly, guinea pigs  
89 vaccinated with BCG-*disA*-OE were significantly better protected against aerosol  
90 challenge with virulent *Mtb* than with BCG-WT suggesting improved protective efficacy  
91 over the existing BCG strain.

92

## 93 **Results**

### 94 **Induction of type I IFN responses by BCG-*disA*-OE**

95 We constructed a recombinant BCG strain (BCG-*disA*-OE) overexpressing the  
96 endogenous diadenylate cyclase gene *disA* (also known as *dacA*) encoded by MT3692  
97 in the CDC1551 genome or Rv3568 in the H37Rv genome. The *disA* genes of *Mtb* and  
98 BCG are 100% identical at the nucleotide level. DisA catalyzes the conversion of 2 ATP  
99 molecules to c-di-AMP (**Supplementary Figure 1a, 1b and 1c**). The overexpression  
100 construct was generated by fusing the *disA* gene to the strong mycobacterial promoter  
101 *hsp60* within the episomal mycobacterial overexpression vector pSD5-*hsp60*. Gene  
102 expression profiling by real time PCR showed ~50-fold upregulation of *disA* expression  
103 in BCG-*disA*-OE as compared to the parental strain (**Supplementary Figure 1d**).

104 Next we evaluated whether strong *disA* expression would result in c-di-AMP-  
105 mediated IRF3 activation and consequent elevations in IFN- $\beta$  levels in mouse  
106 macrophages. Raw Blue™ reporter macrophage cells when infected with BCG-*disA*-OE

107 strains showed a significant 2-fold induction of IRF3 as compared to that observed with  
108 the wild-type parental strain BCG-Pasteur-WT (**Supplementary Figure 2a**). These  
109 preliminary results suggested that heightened levels of c-di-AMP release from  
110 BCG-*disA*-OE produced significant activation of the STING/IRF3 axis, an observation  
111 similar to our earlier findings with *Mtb-disA*-OE [12].

112 Next we infected primary murine BMDMs with BCG-*disA*-OE and BCG-WT and  
113 quantified *Ifnb* gene expression using qPCR. BCG-*disA*-OE-infected macrophages  
114 showed a 2-fold induction of *Ifnb* ( $p < 0.005$ , **Supplementary Fig 2b**) during an early  
115 temporal window. The notion that CDNs such as c-di-AMP can induce STING-dependent,  
116 but c-GAS independent induction of type I IFN responses (even in absence of  
117 extracellular DNA) was validated earlier, and these results were in accordance with our  
118 previous findings with recombinant *M.tb* overexpressing *disA* [12]. Previous studies  
119 suggest that viral infection of non-phagocytic cells lead to cytosolic penetration by leaking  
120 CDNs thus resulting into IFN $\beta$  production [18]. Since BCG lacks a functional Esx-1  
121 secretion system required to release bacterial DNA, these results further reinforce the  
122 idea that phagosomes harboring mycobacteria are rather dynamic leaky structures or  
123 really do not require Esx-1 for membrane disruption [19]. Our data indicate that bacterial-  
124 derived c-di-AMP is detected in the macrophage cytosol and leads to STING-dependent  
125 IFN- $\beta$  synthesis. Increased levels of type I IFNs in macrophages in response to increased  
126 c-di-AMP production in genetically modified BCG was the first step towards generation of  
127 a vaccine strain with an increased antigenic repertoire and ability to stimulate STING.

128

129

## 130 **Macrophage activation by c-di-AMP overexpressing BCG (BCG-*disA*-OE)**

131 Although, the binding affinity of c-di-AMP for STING is weaker than that for  
132 cGAMP, ligation of c-di-AMP with STING appears sufficient to induce co-activation of  
133 transcription factors other than IRF-3 and, hence induction of pro-inflammatory cytokines  
134 [20,21]. Identification of another bona-fide physiological sensor for c-di-AMP, an  
135 endoplasmic adaptor, ERAdP, that binds to c-di-AMP with higher affinity, suggests  
136 ERAdP-dependent initiation of activation of NF- $\kappa$ B signaling in innate immune cells during  
137 bacterial infection [20]. We previously showed that *disA*-OE strains of *M.tb* induce a  
138 strong pro-inflammatory cytokines, such as TNF- $\alpha$ , IL-6 and IL-1 $\beta$ , suggesting  
139 macrophage activation and a complex link between c-di-AMP-based STING activation  
140 and induction of pro-inflammatory cytokines and other interferon stimulated genes (ISGs)  
141 [12]. Bone marrow-derived primary murine macrophages infected with BCG-*disA*-OE  
142 showed significant increased levels of TNF- $\alpha$ , IL-6 and IL-1 $\beta$  in culture supernatants as  
143 compared to uninfected or BCG-WT-infected controls (**Figure 1**). These results reveal a  
144 robust macrophage activation phenotype in response to c-di-AMP overproducing BCG  
145 with increased levels of M1 or Th1 cytokines (TNF- $\alpha$ , IL-1 $\beta$  and IL-6) that is more  
146 pronounced than that seen with BCG-WT.

147

## 148 **CDN-adjuvanted recombinant BCG offers better protection against virulent *M.tb*** 149 **challenge in guinea pigs**

150 Our *in vitro* studies accessing macrophage response due to increased levels of  
151 c-di-AMP encouraged us to test the vaccine potential of BCG-*disA*-OE in the guinea pig  
152 model of tuberculosis infection (**Supplementary Figure 3**). Groups of twelve guinea

153 pigs were vaccinated intradermally with 0.1 ml of PBS (sham vaccination),  $10^5$  CFU of  
154 BCG-*disA*-OE or BCG-WT and held for six weeks before challenge with aerosol  
155 challenge with  $10^2$  CFU of *M. tuberculosis* H37Rv. As described in the Methods, lungs  
156 from one set of infected animals were obtained on day 1 after challenge to confirmed  
157 this implantation dose of *M. tuberculosis* (**Supplementary Figure 4**). Separate groups  
158 of infected animals were euthanized 14 and 18 weeks post-challenge to determine the  
159 protective efficacies of BCG-*disA*-OE and BCG-WT by organ weight, gross pathology,  
160 and bacterial loads in lungs and spleen.

161 At 14-week post-challenge, both BCG-WT and BCG-*disA*-OE vaccinated animals  
162 showed significantly lower lung weight, gross pathology scores, and the bacillary loads  
163 in the lungs, relative to saline-treated controls (**Figure 2A** and **2B**). Vaccination with  
164 BCG-*disA*-OE resulted in the highest reduction in lung gross pathology score, which  
165 was even more pronounced at 18-week post-challenge (**Figure 3A** and **3B**). While the  
166 impact of BCG-*disA*-OE vaccination on lung CFU counts was modest at the 14 week  
167 time point, by the 18 week time point lung CFU counts in the BCG-*disA*-OE vaccinated  
168 guinea pigs were 2.0  $\log_{10}$  units lower than in animals vaccinated with BCG-WT. In  
169 fact, two out of six guinea pigs in BCG-*disA*-OE group had lung CFU counts below the  
170 limit of detection which is ~3-5 bacilli.

171 Additionally, vaccination with BCG-*disA*-OE effectively controlled the  
172 hematogenous spread of *M.tb* to the spleen as evident from significant reduction in  
173 spleen weights, spleen pathology scores, and spleen bacterial burdens when compared  
174 with the sham-immunized animals at both 14 and 18 week post-infection  
175 (**Supplementary Figure 5** and **Figure 4**, respectively). While spleen pathology scores



176 were comparable between animals vaccinated with wild-type and *disA* overexpressing  
177 BCG at 14-weeks post-challenge (**Supplementary Fig 5**), by 18 weeks after challenge  
178 significantly spleen lower pathology scores was observed in the latter group (**Figure 4**).  
179 In addition, there was a trend towards lower spleen CFU in animals vaccinated with  
180 *disA* overexpressing strain compared to BCG, especially when examined at 18-weeks  
181 post-challenge (**Supplementary Figure 4**). Indeed, at 18 weeks post-challenge, three  
182 out of six guinea pigs in BCG-*disA*-OE group had spleen CFU below the limits of  
183 detection. These findings clearly indicate that administration of BCG-*disA*-OE effectively  
184 controlled *M.tb* replication in the lungs and its dissemination to the spleen.

185

## 186 **DISCUSSION**

187 The cytosolic danger sensor STING has emerged as a central Toll-like receptor-  
188 independent mediator of host innate immune responses. STING is activated by binding  
189 CDNs either secreted by bacteria (such as c-di-AMP or c-di-GMP) or distinct host CDNs  
190 (such as cGAMP) generated by host cell receptor following recognition of cytosolic  
191 double-stranded DNA [22-24]. As a relatively new class of immunomodulatory molecules,  
192 CDNs exhibit strong potential to promote protective immunity and increase vaccine  
193 potency through STING-dependent signaling that involve transcription factors IRF-3, IRF-  
194 7 and NF- $\kappa$ B [6,10,11]. STING agonists are therefore regarded as promising immune  
195 adjuvants for promoting immune responses against tumors and infections. However, the  
196 efficacy of small molecule STING agonists as vaccine adjuvants may be limited since they  
197 are rapidly cleared and may not gain long-lived access to the cytosol for STING activation.

198           Here we tested the hypothesis that BCG strains overexpressing the STING agonist  
199 c-di-AMP might offer sustained intracellular delivery of c-di-AMP and thereby improve the  
200 vaccine potential of BCG against TB. We constructed a c-di-AMP-producing  
201 recombinant BCG strain by over-expressing the *disA* (MT3692) gene which is identical at  
202 the nucleotide level in both *M.tb* and BCG. Since BCG survives and replicates  
203 intracellularly for several weeks post-vaccination, over-expression of *disA* under the  
204 influence of strong constitutive mycobacterial *hsp60* promoter allows sustained  
205 intracellular exposure of the STING agonist in the cytosol of phagocytic cells. By utilizing  
206 BCG as the vector for STING agonist delivery, BCG-*disA*-OE offers enhanced innate  
207 immune activation via the STING pathways in addition to the full antigenic repertoire of  
208 BCG.

209           Complex genomic rearrangements in BCG strains are one of the major  
210 contributors of immunological and phenotypic differences that in turn contribute to the  
211 variability in the degree of protection offered by BCG [16,25]. A global resurgence of  
212 MDR-TB, HIV-TB co-infection has heightened the need for an improved TB vaccine that  
213 provides better protection than that of BCG. Additionally, new vaccines must be safe  
214 enough to be used in immunocompromised HIV-TB co-infected individuals. Rational  
215 modification of live BCG to increase its antigenic repertoire, and with a prior knowledge  
216 of attenuation factors and immunity is critically needed [14,17]. While our study did not  
217 directly assess the virulence of BCG-*disA*-OE to that of BCG-WT, based on the finding  
218 that *Mtb-disA*-OE showed a median time to death in BALB-c mice of 321.5 days compared  
219 to 150.5 days for *Mtb*-WT following an aerosol infection of 3.5 log<sub>10</sub> CFU [12], we  
220 anticipate that BCG-*disA*-OE is a weaker pathogen than BCG-WT.

221           Inside the host, both CD4+ and CD8+ T cells are essential for protective immunity  
222 against TB. Dendritic cells (DCs) migrating from the alveoli to the draining lymph nodes  
223 are crucial for activation of *M.tb* antigen-specific CD4+ and CD8+ T cells and contribute  
224 to resistance to *M.tb* [26]. The requirement for a Th1-like T cells response for host  
225 immunity against *M.tb* is clear, and recent vaccine development has sought to stimulate  
226 both CD4 and CD8 T-cell responses to produce Th1 cytokines [15]. Hence, elicitation of  
227 enduring Th1 responses is a desirable feature of candidate TB vaccines. Not only are  
228 STING-activating adjuvants known to elicit antigen-specific Th1 responses, but they also  
229 elicit Th17 responses and have been shown to confer improved protection against *M.tb*  
230 [10,27]. A recent report published while this manuscript was in preparation suggested that  
231 the protection efficacy of protein subunit vaccine adjuvanted with small molecule CDNs  
232 was durable for up to 12 weeks after *M.tb* challenge in mice, suggesting that a CDN-  
233 adjuvanted vaccine can reduce TB progression in mice through T cell-dependent  
234 mechanisms [27].

235           Guinea pigs are highly susceptible to *M.tb* infection, and the model provides an  
236 important pre-clinical evaluation of potential vaccine candidates [28]. Immunization with  
237 a single dose of BCG-*disA*-OE resulted in a marked reduction in the gross pathology and  
238 bacterial loads in both lungs and spleens of *M.tb* challenged animals when compared to  
239 sham treatment or vaccination with BCG alone. Thus our studies highlight the improved  
240 potential of BCG-*disA*-OE over BCG to impart protection against *M.tb* infection and  
241 disease dissemination.

242

243           This study is an important step forward towards implementing CDN-based STING  
244 agonists as novel vaccine adjuvants into vaccine strategies for TB. Our results provide  
245 proof-of-concept data for utilizing BCG as the vector for producing STING agonist(s)  
246 naturally from within the intracellular compartment in a sustained fashion. Our results  
247 suggest that STING agonist overexpressing BCG may offer greater efficacy as TB  
248 vaccine than BCG alone and that this approach may have utility as an immunotherapeutic  
249 tool against other diseases including cancer.

250

## 251 **MATERIALS AND METHODS**

252 **Animals:** All procedures involving live animals were performed in agreement with the  
253 protocols approved by the Institutional Animal Care and Use Committee at the Johns  
254 Hopkins University School of Medicine. Pathogen-free female outbred guinea pigs (300  
255 g) and C57BL/6 mice were purchased from Charles River Laboratories (North  
256 Wilmington, Mass.). Uninfected guinea pigs were housed under pathogen-free conditions  
257 at BSL3 animal facility without cross-ventilation. C57BL/6J mice were housed in BSL2  
258 animal facility at the School of Medicine, Johns Hopkins University. Animals were given  
259 free access to water and standard mouse or guinea pig chow, respectively. The general  
260 behavior and appearance were monitored by veterinary specialists.

261 **Bacterial strains and cell culture:** Details of all bacterial strains are provided in  
262 **Supplementary Table 1**. BCG Pasteur was the kind gift of Frank Collins from the FDA,  
263 and *M. tuberculosis* H37Rv and CDC1551 were obtained from ATCC. Frozen vials of  
264 bacterial strains were revived and subsequently sub-cultured in 7H9 Middlebrook liquid  
265 medium (B271310, Fisher Scientific) supplemented with oleic acid-albumin-dextrose-

266 catalase (OADC) (B11886, Fisher Scientific), 0.5% glycerol (G5516, Sigma) and 0.05%  
267 Tween-80 (BP338, Fisher Scientific) in BSL3 facility. Murine bone marrow was isolated  
268 from 4-6 weeks old female C57BL/6J mice. Approximately  $10^8$  cells were stored in  
269 cryopreservation media made of 10% DMSO (D2650, Sigma) in heat inactivated FBS  
270 (10082-147, Fisher Scientific) overnight at  $-80^{\circ}\text{C}$  followed by transfer to deep  
271 cryopreservation in liquid nitrogen. For differentiation of bone marrow cells into primary  
272 macrophages, bone marrow cells were differentiated for 7 days in presence of RPMI-  
273 Glutamax (61870-036, Fisher Scientific) supplemented with 10% heat inactivated fetal  
274 bovine serum and antibiotics (Penicillin-Streptomycin solution) (15140-122, Fisher  
275 Scientific) and 30% (vol/vol) L929 conditioned media. Mouse fibroblast L929 cells  
276 (ATCC® CCL-1™) were maintained in RPMI-1640 medium supplemented with 10% FBS  
277 and antibiotics.

278 **Overexpression of MT3692 in BCG Pasteur:** High molecular weight genomic DNA was  
279 isolated using CTAB method from log phase cultures of *M.tb*-CDC 1551. Using gene-  
280 specific primers (**Supplementary Table 2**), pSD5hsp60.MT3692 (F) and  
281 pSD5hsp60.MT3692 (R), the *disA* (MT3692) gene of *M.tb*, was PCR amplified from *M.tb*-  
282 derived genomic DNA. Gene amplicons were cloned into mycobacterial shuttle vector  
283 pSD5-hsp60 (**Supplementary Table 1**) at the NdeI and MluI restriction sites. The clone  
284 (pSD5-hsp60-MT3692) was confirmed by insert release and sequence analyses. The  
285 construct pSD5-hsp60-MT3692 was subsequently used to transform BCG.  
286 Recombinants clones (BCG-*disA*-OE) selected against kanamycin (25  $\mu\text{g}/\text{mL}$ ) and further  
287 conformed using colony PCR using kanamycin-specific primers (**Supplementary Table**

288 **2).** MT3692 overexpression phenotype of BCG-*disA*-OE strain was further confirmed by  
289 mRNA expression using quantitative real time PCR (qPCR).

290 **Quantitative real-time PCR (qPCR):** Late log phase BCG culture pellets were bead  
291 beaten using Zirconium beads (KT03961-1-102.BK, Berlin Technologies) before  
292 performing total RNA isolation. Trizol reagent (15596026, Fisher Scientific) was used for  
293 RNA isolation from both bacterial and mammalian cells. Quantification of mRNA,  
294 amplification, and quantification of cDNA was carried out using SYBR Fast green double  
295 stranded DNA binding dye (4085612, Applied Biosystems, USA) and ABI StepOnePlus  
296 Real Time PCR System (Applied Biosystems, USA). Amplification of *sigH* and mouse  
297 beta actin was used as internal controls for BCG and mouse BMDMs respectively. Melt  
298 curve analyses confirmed formation of desired and specific PCR product. Experiments  
299 were performed in triplicate using three independent biological samples and results were  
300 analyzed and presented using  $2^{-\Delta\Delta CT}$  method. Details of NCBI gene identifiers and primer  
301 sequences are mentioned (**Supplementary Table 2**).

302 **Macrophage infection, IRF3 activation assay and cytokine ELISAs:** Infection assays  
303 were performed in resting mouse BMDMs in 24 well plates in triplicates. Briefly, early log-  
304 phase cultures of BCG strains were washed, diluted appropriately to pre-defined  
305 concentrations using macrophage infection media (DMEM with 10% FBS) and deposited  
306 on the monolayer of cells at a precalibrated MOI (1:20). Infection was allowed continue  
307 for 5 h, following which uninfected extracellular bacilli were removed by repeated washing  
308 using Dulbecco's PBS (DPBS). This time point was considered 0 h and the cells were  
309 incubated for desired number of hours till the end points were met. To access accurate  
310 bacterial counts of infection and internalized bacterial numbers, serial dilutions of the

311 bacterial suspension and 0.025% SDS lysed macrophage were plated on 7H9 plates.  
312 RAW-Blue ISG (InvivoGen) reporter cells, derived from the murine RAW 264.7  
313 macrophage cell line by stably integrating an interferon regulatory factor (IRF)-inducible  
314 secreted embryonic alkaline phosphatase (SEAP) reporter construct were used for IRF  
315 activation assay. The cells were infected with wild-type and BCG-*disA*-OE strains. Cells  
316 were incubated for 18 h in fresh macrophage infection media (DMEM with 10% FBS), and  
317 culture supernatants were harvested for determination of IRF activation by a SEAP  
318 colorimetric assay using QUANTI-Blue reagent (InvivoGen). Following macrophage  
319 infection, culture supernatants were isolated, filtered and immediately frozen at -80 for  
320 cytokine quantification. Mouse DuoSet ELISA kits for TNF (DY410), IL-6 (DY206-05) and  
321 IL1 $\beta$  (DY201-05) were used for cytokine quantification. The absolute concentrations were  
322 determined by referring to a standard curve and expressed as pg/mL. For quantification  
323 experiments were performed in triplicates.

324 **Guinea pig immunization and determination of protective efficacy:** To test the  
325 prophylactic potential of BCG-*disA*-OE as a vaccine candidate, guinea pigs (n=12 per  
326 group) were immunized intradermally using 10<sup>5</sup> cfu/100  $\mu$ l of wild-type parental BCG  
327 Pasteur or BCG-*disA*-OE strains. Guinea pigs were sham immunized with saline. Animals  
328 were challenged with ~100 cfu of *M.tb* H37Rv strain by the aerosol route 6 weeks  
329 **(Supplementary Figure 1)** after primary immunization. Lungs from one set of infected  
330 animals were harvested, and homogenates were plated on day 1 after to check for  
331 established implantation. Infected animals from each group were euthanized 14 and 18  
332 weeks later to determine the protective efficacy of the BCG-*disA*-OE. Gross-pathological  
333 features and bacillary burden in lungs and spleen of sham and BCG-immunized guinea

334 pigs after *M.tb* challenge were measured as described previously [29] . **Supplementary**  
335 **Figure 3** shows the details of experimental plan and different animal groups used in the  
336 study and **Supplementary Table 1** depicts the bacterial strains and plasmid used in the  
337 study.

338 **Statistical analyses:** Fold-expression (qRT-PCR and ELISA) were represented as mean  
339 value  $\pm$  standard error mean (SEM). Differences between individual test groups were  
340 analyzed using by applying unpaired Student's t-test. All statistics was performed using  
341 GraphPad Prism Version 5.01. P values  $< 0.05$  were considered statistically significant.

342

#### 343 **ACKNOWLEDGEMENT**

344 The authors thank Dr. Geetha Srikrishna for help with manuscript writing and editing. This  
345 work was funded by National Institutes of Health grant R01-AI037856 and HL133190 to  
346 W. Bishai.

#### 347 **REFERENCES**

- 348 1 Li, T. and Chen, Z.J. (2018) The cGAS-cGAMP-STING pathway connects DNA  
349 damage to inflammation, senescence, and cancer. *J. Exp. Med.* 215, 1287–1299
- 350 2 Paludan, S.R. and Bowie, A.G. (2013) Immune sensing of DNA. *Immunity* 38, 870–  
351 880
- 352 3 Burdette, D.L. *et al.* (2011) STING is a direct innate immune sensor of cyclic di-GMP.  
353 *Nature* 478, 515–518
- 354 4 Yin, Q. *et al.* (2012) Cyclic di-GMP sensing via the innate immune signaling protein  
355 STING. *Mol. Cell* 46, 735–745
- 356 5 McCaffary, D. (2017) STING signalling: an emerging common pathway in  
357 autoimmunity and cancer. *Immunopharmacol. Immunotoxicol.* 39, 253–258



- 358 6 Dubensky, T.W. *et al.* (2013) Rationale, progress and development of vaccines  
359 utilizing STING-activating cyclic dinucleotide adjuvants. *Ther. Adv. Vaccines* 1, 131–  
360 143
- 361 7 Iurescia, S. *et al.* (2018) Targeting Cytosolic Nucleic Acid-Sensing Pathways for  
362 Cancer Immunotherapies. *Front. Immunol.* 9, 711
- 363 8 Li, X.-D. *et al.* (2013) Pivotal roles of cGAS-cGAMP signaling in antiviral defense and  
364 immune adjuvant effects. *Science* 341, 1390–1394
- 365 9 Libanova, R. *et al.* (2010) The member of the cyclic di-nucleotide family bis-(3', 5')-  
366 cyclic dimeric inosine monophosphate exerts potent activity as mucosal adjuvant.  
367 *Vaccine* 28, 2249–2258
- 368 10 Ebensen, T. *et al.* (2011) Bis-(3',5')-cyclic dimeric adenosine monophosphate: strong  
369 Th1/Th2/Th17 promoting mucosal adjuvant. *Vaccine* 29, 5210–5220
- 370 11 Libanova, R. *et al.* (2012) Cyclic di-nucleotides: new era for small molecules as  
371 adjuvants. *Microb. Biotechnol.* 5, 168–176
- 372 12 Dey, B. *et al.* (2015) A bacterial cyclic dinucleotide activates the cytosolic surveillance  
373 pathway and mediates innate resistance to tuberculosis. *Nat. Med.* 21, 401–406
- 374 13 Dey, R.J. *et al.* (2017) Inhibition of innate immune cytosolic surveillance by an *M.*  
375 *tuberculosis* phosphodiesterase. *Nat. Chem. Biol.* 13, 210–217
- 376 14 Kaufmann, S.H.E. (2014) Tuberculosis vaccine development at a divide. *Curr. Opin.*  
377 *Pulm. Med.* 20, 294–300
- 378 15 Ablasser, A. *et al.* (2013) Cell intrinsic immunity spreads to bystander cells via the  
379 intercellular transfer of cGAMP. *Nature* 503, 530–534
- 380 16 Conrad, W.H. *et al.* (2017) Mycobacterial ESX-1 secretion system mediates host cell  
381 lysis through bacterium contact-dependent gross membrane disruptions. *Proc. Natl.*  
382 *Acad. Sci. U. S. A.* 114, 1371–1376
- 383 17 Xia, P. *et al.* (2018) The ER membrane adaptor ERAdP senses the bacterial second  
384 messenger c-di-AMP and initiates anti-bacterial immunity. *Nat. Immunol.* 19, 141–150
- 385 18 Rivera Vargas, T. *et al.* (2017) Rationale for stimulator of interferon genes-targeted  
386 cancer immunotherapy. *Eur. J. Cancer Oxf. Engl.* 1990 75, 86–97
- 387 19 Burdette, D.L. and Vance, R.E. (2013) STING and the innate immune response to  
388 nucleic acids in the cytosol. *Nat. Immunol.* 14, 19–26

- 389 20 Diner, E.J. *et al.* (2013) The innate immune DNA sensor cGAS produces a  
390 noncanonical cyclic dinucleotide that activates human STING. *Cell Rep.* 3, 1355–  
391 1361
- 392 21 Ablasser, A. *et al.* (2013) cGAS produces a 2'-5'-linked cyclic dinucleotide second  
393 messenger that activates STING. *Nature* 498, 380–384
- 394 22 Zhang, L. *et al.* (2016) Variable Virulence and Efficacy of BCG Vaccine Strains in Mice  
395 and Correlation With Genome Polymorphisms. *Mol. Ther. J. Am. Soc. Gene Ther.* 24,  
396 398–405
- 397 23 Brosch, R. *et al.* (2007) Genome plasticity of BCG and impact on vaccine efficacy.  
398 *Proc. Natl. Acad. Sci. U. S. A.* 104, 5596–5601
- 399 24 Martin, C. (2006) Tuberculosis vaccines: past, present and future. *Curr. Opin. Pulm.*  
400 *Med.* 12, 186–191
- 401 25 Cooper, A.M. (2009) Cell-mediated immune responses in tuberculosis. *Annu. Rev.*  
402 *Immunol.* 27, 393–422
- 403 26 Martín, C. (2005) The dream of a vaccine against tuberculosis; new vaccines  
404 improving or replacing BCG? *Eur. Respir. J.* 26, 162–167
- 405 27 Van Dis, E. *et al.* (2018) STING-Activating Adjuvants Elicit a Th17 Immune Response  
406 and Protect against *Mycobacterium tuberculosis* Infection. *Cell Rep.* 23, 1435–1447
- 407 28 Clark, S. *et al.* (2014) Animal models of tuberculosis: Guinea pigs. *Cold Spring Harb.*  
408 *Perspect. Med.* 5, a018572
- 409 29 Jain, R. *et al.* (2008) Enhanced and enduring protection against tuberculosis by  
410 recombinant BCG-Ag85C and its association with modulation of cytokine profile in  
411 lung. *PloS One* 3, e3869

412

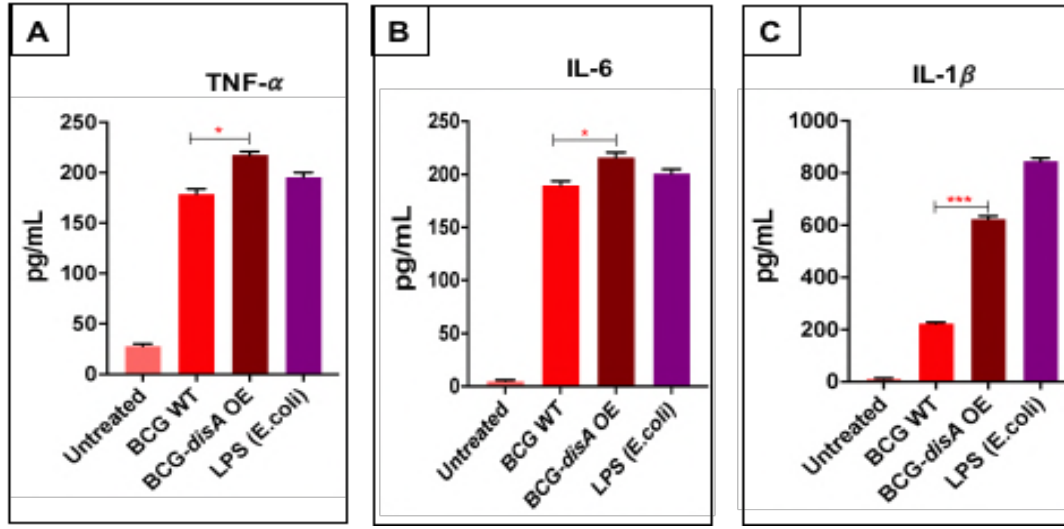
413

414

415

416

Figure 1



417

418 **Figure 1. Modulation of pro-inflammatory cytokines in response to *disA***

419 **overexpression.** Differential induction of (a) TNF- $\alpha$ , (b) IL-6 and (c) IL1 $\beta$  in mouse

420 BMDMs challenged with wild-type and *disA* overexpression strains of *Mycobacterium*

421 *bovis* BCG-Pasteur. BMDMs were challenged with wild-type and *disA* OE strains at an

422 MOI of 1:20 for 5 h to establish the infection. Uninfected bacteria were washed using ice-

423 cold DPBS and cells were subsequently incubated for another 24 h. Culture supernatants

424 were assayed by ELISA for different cytokines. The graphical points represent mean of 3

425 independent experiments  $\pm$  standard error mean (SEM). Student's t test (\*P < 0.05 \*\*P <

426 0.01, \*\*\*P < 0.001). MOI (multiplicity of infection).

427

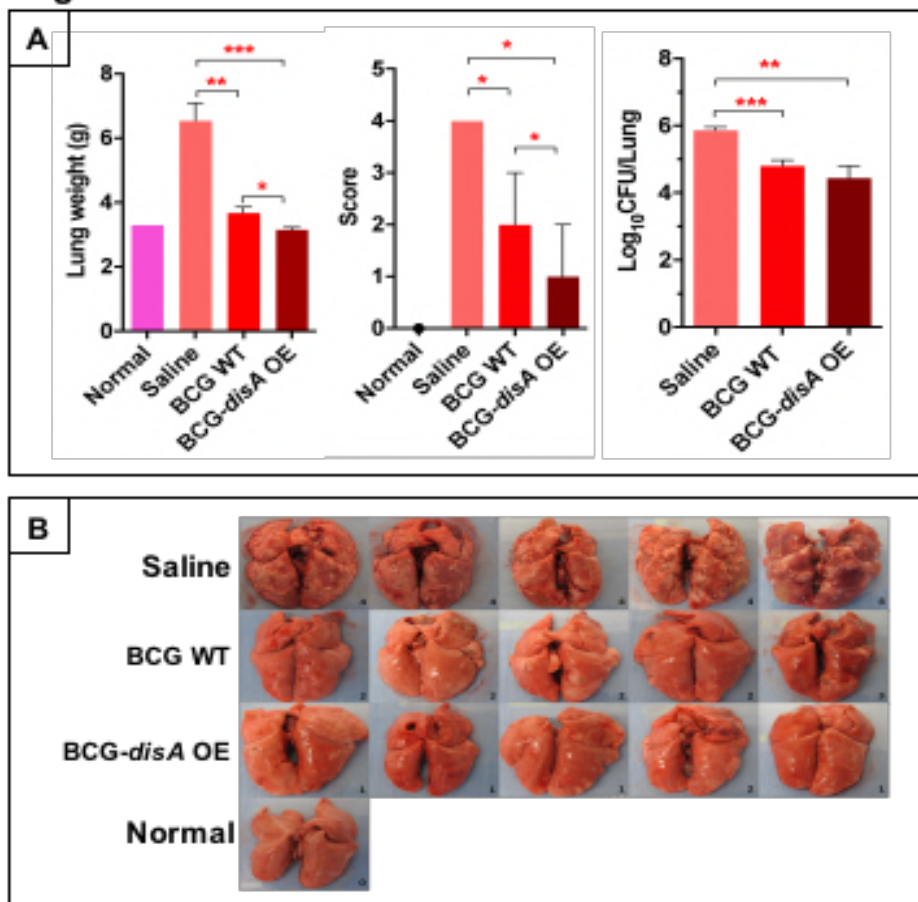
428

429

430

431

**Figure 2**



432

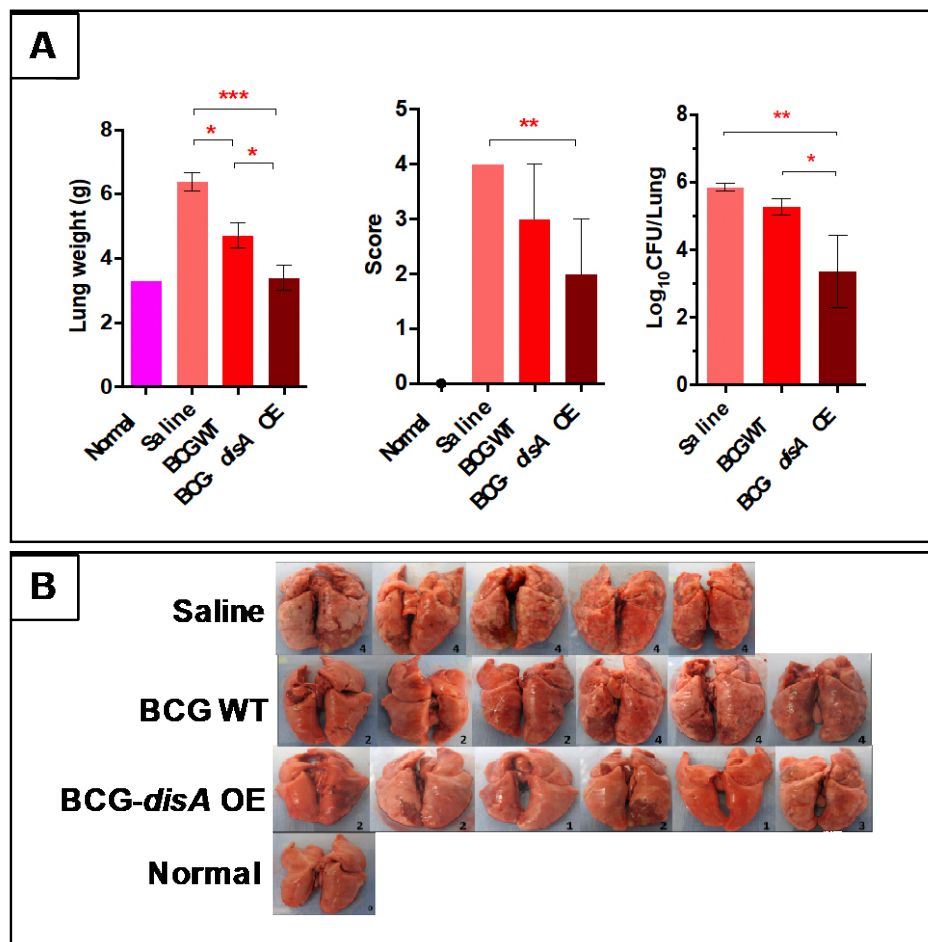
433 **Figure 2. Effect on lung weight, gross lung pathology scores and lung gross-**  
434 **morphological features in guinea pigs 14 weeks post-challenge with *M.***  
435 ***tuberculosis* H37Rv following vaccination with BCG-WT or BCG-disA-OE. A) Lung**  
436 **weights and gross pathology scores at 14 weeks post-*M. tuberculosis* challenge. B)**  
437 **Images of lungs at necropsy. \*\*\*P < 0.001, \*\*, P< 0.01; \*, P<0.05; Non-parametric Man**  
438 **Whitney Test.**

439

440

441

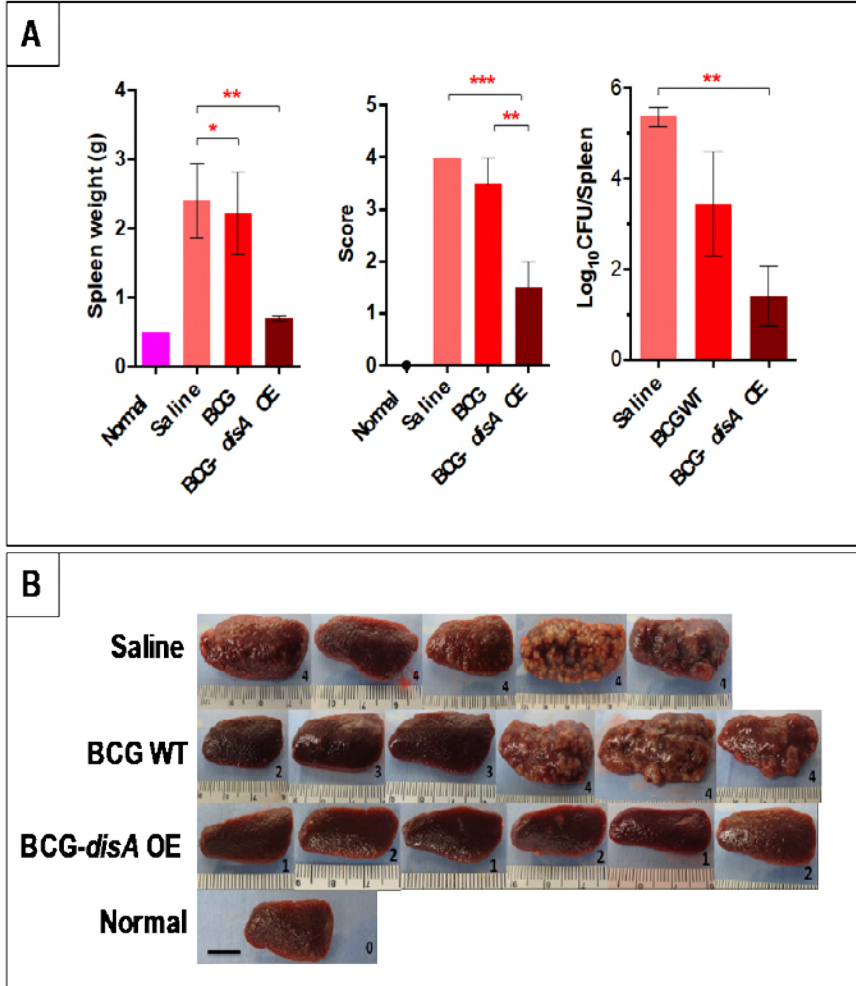
**Figure 3**



442  
443  
444  
445  
446  
447  
448  
449  
450  
451  
452  
453  
454

**Figure 3. Effect on lung weight, gross lung pathology scores, bacterial burden, and lung gross-morphological features in guinea pigs 18 weeks post-challenge with *M. tuberculosis* H37Rv following vaccination with BCG-WT or BCG-*disA*-OE.** A) Lung weights, gross pathology scores, and *M. tuberculosis* bacterial burden at 18 weeks post-*M. tuberculosis* challenge. Two guinea pigs in BCG-*disA*-OE group had lung CFU counts below the limit of our detection. B) Images of lungs at necropsy. \*\*\*P < 0.001, \*\*, P < 0.01; \*, P < 0.05; Non-parametric Man Whitney Test.

**Figure 4**

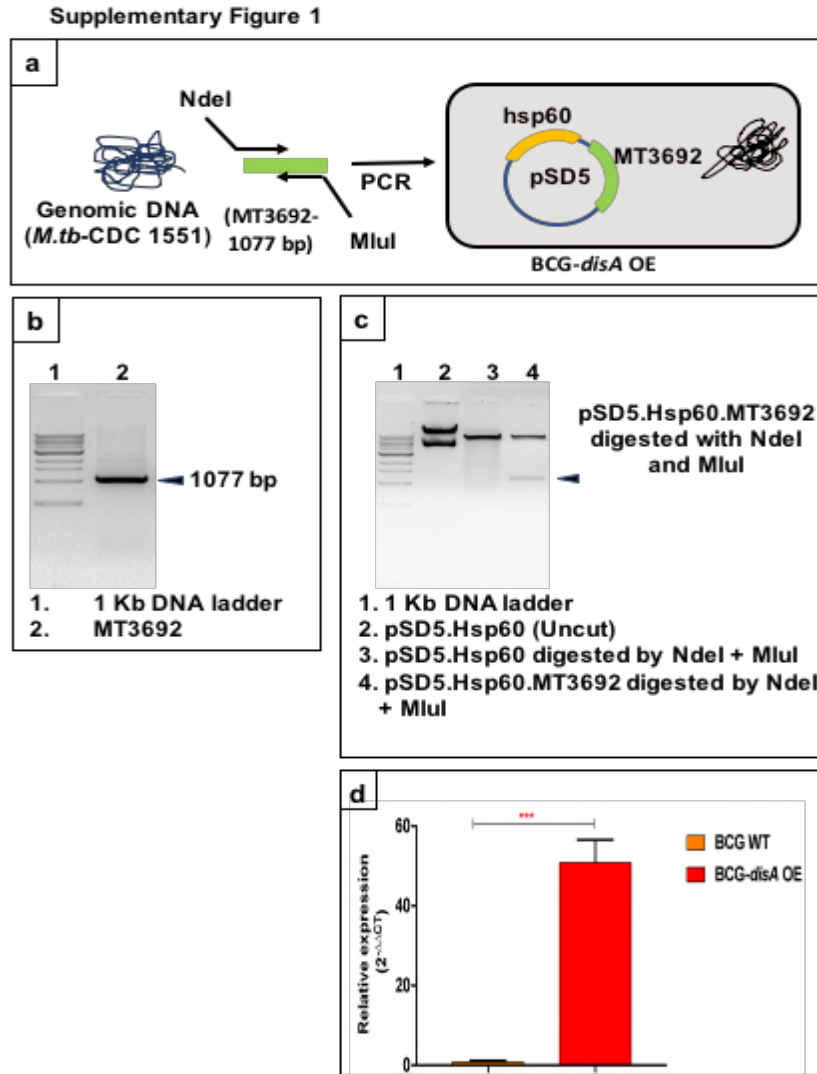


455  
456  
457  
458  
459  
460  
461  
462  
463  
464  
465

**Effect on spleen weight, gross spleen pathology scores, bacterial burden, and spleen gross-morphological features in guinea pigs 18 weeks post-challenge with *M. tuberculosis* H37Rv following vaccination with BCG-WT or BCG-*disA*-OE.** A) Spleen weights, gross pathology scores, and *M. tuberculosis* CFU counts at 18 weeks post-*M. tuberculosis* challenge. Three guinea pigs in BCG-*disA*-OE group had spleen CFU counts below the limit of our detection. B) Images of spleens at necropsy. Scale bars indicate 1 cm. The number in the box is gross pathological score. \*\*\* $P < 0.001$ , \*\*,  $P < 0.01$ ; \*,  $P < 0.05$ ; Non-parametric Man Whitney Test.

466 **SUPPLEMENTARY FIGURES AND TABLES**

467



468

469 **Supplementary Figure 1. Generation of the BCG-*disA*-OE strain and confirmation**

470 **of c-di-AMP overexpression. (a)** The MT3692 (*disA*) gene of *M. tuberculosis* was PCR-

471 amplified from *M. tuberculosis* CDC 1551 genomic DNA using gene-specific cloning

472 primers. **(b)** The amplicons were cloned into the mycobacterial shuttle expression vector

473 pSD5-hsp60 at the NdeI and MluI restriction sites. The construct (PSD5-*hsp60*-MT3692)

474 generation was confirmed using restriction analyses and sequencing. Constructs were



475 used to transform wild-type BCG Pasteur strain and recombinant clones were selected  
476 against Kanamycin (25 µg/mL). **(c)** Differential expression of *disA* in wild-type and  
477 BCG-*disA*-OE strains. Gene expression was measured in total RNA isolated from the late  
478 log phase cultures using SYBR based quantitative real-time PCR. The graphical data  
479 points represent the mean of 3 independent experiments ± standard error mean (SEM).  
480 *M. tuberculosis sigA* (Rv2703) was used an internal control. Data analysis was performed  
481 using  $2^{-\Delta\Delta CT}$  method. Student's t test (\*\*P < 0.0001).

482

483

484

485

486

487

488

489

490

491

492

493

494

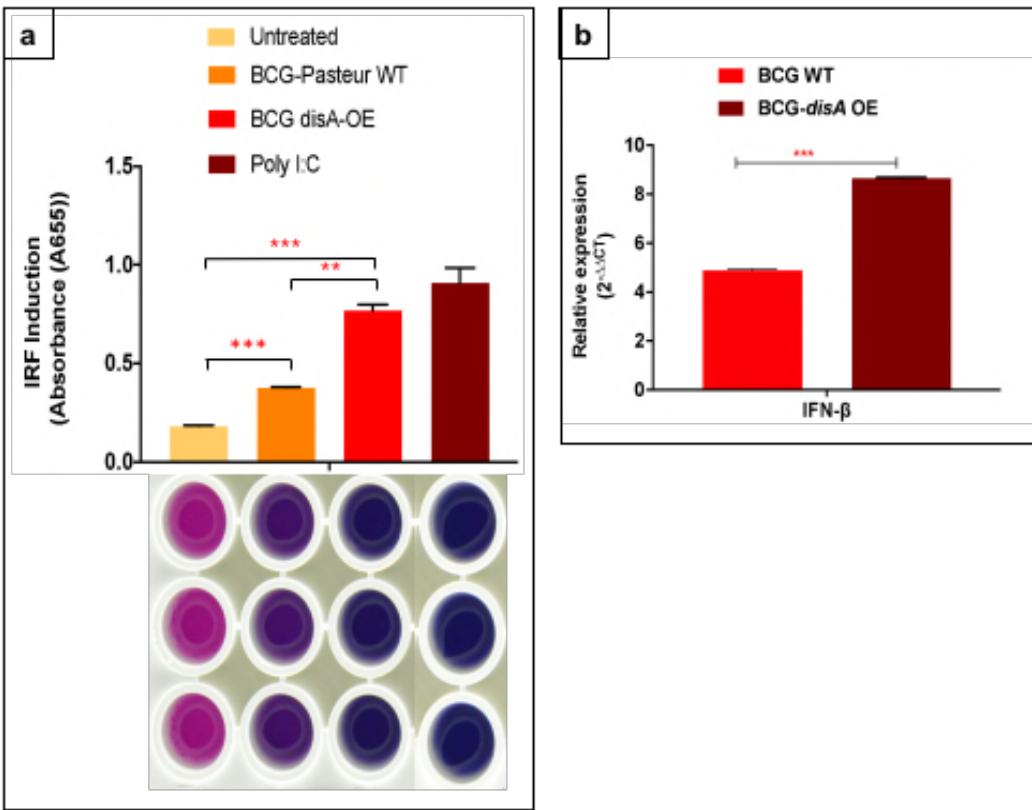
495

496

497



## Supplementary Figure 2



498

499 **Supplementary Figure 2. BCG-*disA*-OE overexpressing c-di-AMP gives more**

500 **potent IRF3 and Type I IFN stimulation that BCG-WT: (a) Effect of *disA* overexpression**

501 on activation of IRF pathway measured by IRF-SEAP QUANTI Blue reporter assay.

502 RAW-Blue ISG cells were challenged with wild-type and BCG-*disA*-OE strains at an MOI

503 of 1:20 for 5 hours to establish the infection. Uninfected bacteria were washed out using

504 ice-cold DPBS and subsequently incubated for another 18-24 hours. The culture

505 supernatants of infected RAW-Blue ISG cells were assayed for IRF activation. The image

506 below the IRF-activation graph represents QUANTI Blue assay plate and sample wells;

507 treatment parameters for column of wells correspond to those defined for the bars above

508 aligned with the wells. The graphical points represent mean of three independent

509 experiments  $\pm$  standard error mean (SEM). Student's t test (\*\*P < 0.0005, \*\*P < 0.001).

510 **(b)** Differential expression of IFN $\beta$ : Mouse BMDMs were challenged with wild-type and  
511 BCG-*disA*-OE strains at an MOI of 1:20 for 5 hours to establish the infection. Uninfected  
512 bacteria were washed using ice-cold DPBS and cells were subsequently incubated for  
513 another 6 hours. Expression levels of mRNA was measured using a SYBR green-based  
514 quantitative real-time PCR. Basal level of transcript (mRNA) in untreated macrophages  
515 was used for data normalization and hence to access relative expression.  $\beta$ -actin was  
516 used as an internal control. Data analysis was performed using  $2^{-\Delta\Delta CT}$  method. The  
517 graphical points represent mean of 3 independent experiments  $\pm$  standard error mean  
518 (SEM). Student's t test (\*\*P < 0.0005, \*\*P < 0.001). MOI (multiplicity of infection).

519

520

521

522

523

524

525

526

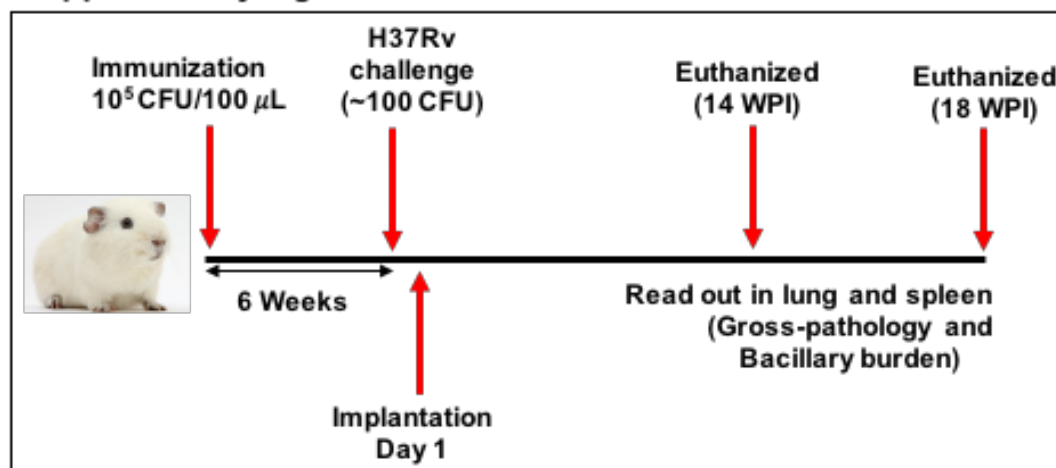
527

528

529

530

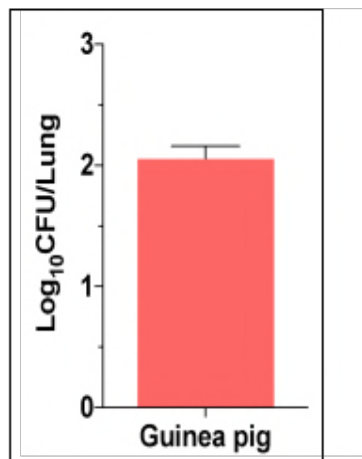
### Supplementary Figure 3



531  
532 **Supplementary Figure 3.** Time line showing the experimental strategy of BCG  
533 immunization and challenge in the guinea pig model of vaccination followed by *M.*  
534 *tuberculosis* aerosol infection challenge.

535  
536  
537  
538  
539  
540  
541  
542  
543  
544  
545  
546  
547

#### Supplementary Figure 4



548

549 **Supplementary Figure 4 Bacillary load in the guinea pig lung following *M.***

550 ***tuberculosis* challenge.** The bacillary load in the lung of guinea pigs (n=3) were

551 determined at day 1 post aerosol challenge. Briefly, animals were euthanized, and lungs

552 were aseptically removed and homogenized in saline. The homogenates were serially

553 diluted and plated in duplicates on 7H11 medium supplemented with appropriate

554 antibiotics. To determine colony forming unit (CFU), Log<sub>10</sub> CFU were graphically

555 represented as dot plot, wherein median values ± standard error mean (SEM) are

556 denoted by horizontal line.

557

558

559

560

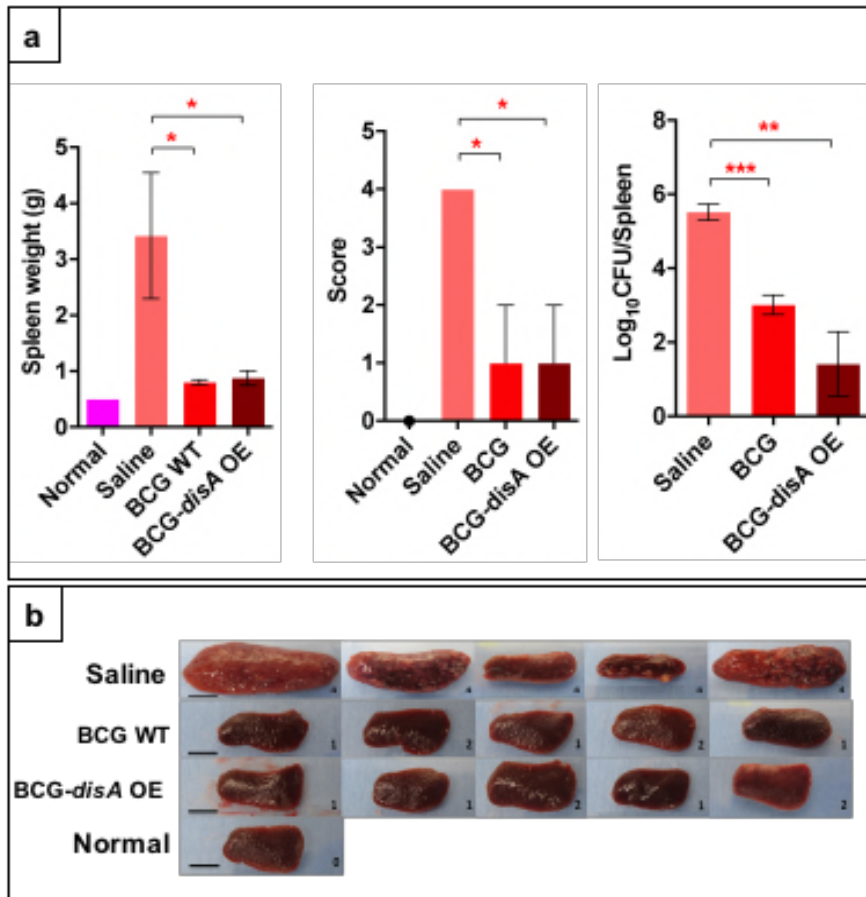
561

562

563

564

## Supplementary Figure 5



565

566 **Supplementary Figure 5.**

567 **Effect on spleen weight, gross spleen pathology scores, bacterial burden, and**  
568 **spleen gross-morphological features in guinea pigs 14 weeks post-challenge with**  
569 ***M. tuberculosis* H37Rv following vaccination with BCG-WT or BCG-*disA*-OE. A)**  
570 **Spleen weights, gross pathology scores, and *M. tuberculosis* CFU counts at 14 weeks**  
571 **post-*M. tuberculosis* challenge. B) Images of spleens at necropsy. Scale bars indicate 1**  
572 **cm. The number in the box is gross pathological score. \*\*, P< 0.01; \*, P<0.05; Non-**  
573 **parametric Man Whitney Test.**

574

575

576 **Supplementary Table 1: Bacterial strains and plasmids used in this study**

Name	Description
<b><i>M. tuberculosis</i> strains</b>	
Mtb-CDC1551	Wild-type <i>M. tuberculosis</i>
<i>Mtb</i> -H37Rv	Wild-type <i>M. tuberculosis</i>
<b><i>M. bovis</i> BCG strains</b>	
BCG	<i>M. bovis</i> BCG Pasteur
BCG- <i>disA</i> -OE	BCG Pasteur strain overexpressing <i>disA</i> (MT3692) of <i>M.tb</i>
<b>Plasmids</b>	
pSD5.hsp60	Mycobacterial expression plasmid with hsp60 promoter
pSD5hsp60.MT3692	<i>disA</i> over-expression plasmid

577  
578 **Supplementary Table 2: Cloning and PCR primers used in the study**  
579

<b>List of primer sequences used for gene expression analysis</b>		
Accession Number	Gene	Primer Sequence 5'-3'
	pSD5hsp60.MT3692 (F)	GGGCATCATATGCACGCTGTGACTCGTC
	pSD5hsp60.MT3692 (R)	GGGACGCGTTATTGATCGCTGATGGTCG ATT
	Kanamycin cassette (F)	GAGAAACTCACCGAGGCAG
	Kanamycin cassette (R)	GTATTTTCGTCTCGCTCAGGC
32287254	<i>M.tb</i> sigH (F)	GCGATGGTGGCTTCTCCCTCG
	<i>M.tb</i> sigH (R)	CCATCTTGACACAGCTCGCGTAG
11461	Mouse.β actin (F)	TAAGGCCAACCGTGAAAAGATG
	Mouse.β actin (R)	CTGGATGGCTACGTACATGGCT
15977	Mouse. IFNβ (F)	CCACAGCCCTCTCCATCAAC
	Mouse. IFNβ (R)	CTCCGTCATCTCCATAGGGA
922803	<i>M.tb-disA</i> (F)	GCGATGGTGGCTTCTCCCTCG
	<i>M.tb-disA</i> (R)	CCATCTTGACACAGCTCGCGTAG

580